Carbon nanotubes on Jurkat cells: effects on cell viability and plasma membrane potential

2008 J. Phys.: Condens. Matter 20 474204

(http://iopscience.iop.org/0953-8984/20/47/474204)

J. Phys.: Condens. Matter **20** (2008) 474204 (9pp) doi:10.1088/0953-8984/20/47/474204

Carbon nanotubes on Jurkat cells: effects on cell viability and plasma membrane potential

Milena De Nicola[1], Stefano Bellucci[2,4], Enrico Traversa[3], Giovanni De Bellis[2], Federico Micciulla[2] and Lina Ghibelli[1]

[1] Department of Biology, University of Rome 'Tor Vergata', Italy
[2] INFN-Laboratori Nazionali di Frascati, Italy
[3] Department of Chemical Science and Technology, University of Rome 'Tor Vergata', Italy

E-mail: bellucci@lnf.infn.it

Received 24 April 2008
Published 6 November 2008
Online at stacks.iop.org/JPhysCM/20/474204

Abstract

Carbon nanotubes (CNT) are one of the most novel attractive materials in nanotechnology for their potential multiple applications, including in the biomedical fields. The biocompatibility and toxicity of these novel nanomaterials are still largely unknown and a systematic study on biological interference is essential. We present a toxicological assessment of different types of CNT on the human tumor lymphocytic Jurkat cells. The carbon nanomaterials examined differ in preparation, size, contaminants and morphology: (1) CNT composed of MWCNT + SWCNT, with no metal contaminants; (2) MWCNT and (3) SWCNT, both with metal contaminants; (4) carbon black as control. The results indicate that CNT exert a dose- and time-dependent cytotoxic effect on Jurkat cells, inducing apoptotic cell death, accelerating the transition to secondary necrosis and increasing the extent of apoptosis induced by damaging agents; interestingly, CNT induce a plasma membrane hyperpolarization. These alterations are produced by all types of CNT, but contaminants and/or the size modulate the extent of such effects. Thus CNT deeply affect cell behavior, suggesting that they might play a role in inflammation, and recommending greater attention in terms of evaluation of exposure risks.

(Some figures in this article are in colour only in the electronic version)

1. Introduction

Carbon nanotubes (CNT) are considered one of the most novel attractive materials in nanotechnology. Their extraordinary electrical, mechanical and thermal characteristics point towards many technological applications. The different synthesis, purification and post-processing methods produce CNT with different physical characteristics, which can be applied in many different fields ranging from energy storage devices [1]to high resistance composites [2] to electronic devices [3].

The intense research into new nanotechnology applications provides an extraordinary amount of novel materials with respect to the effort posed so far on the health risks of these engineered nanoparticles. Due to the explosive increase in CNT mass production, toxicological studies are required to prevent possible health hazards among workers involved in the research and manufacture of these materials, and in the general public [4].

CNT have generated extraordinary interest and expectations also for biomedical applications [5, 6].

CNT may be functionalized with various chemical groups, peptides, proteins or, in general, specific target molecules, to develop delivery systems for chemicals and drugs that can move through the body to target cells [4, 7–13]. Extremely interesting biotechnological applications come from the possibility that CNT may also be used as components of tissue scaffolds to promote cell proliferation and differentiation [14, 15]. These new potential applications call for thorough studies on biocompatibility and toxicological

[4] Author to whom any correspondence should be addressed.

burden. The identification of possible risks to human health is an essential prerequisite for a successful introduction of CNT in future technological and biomedical applications.

The literature on the health effects of CNT suggests their potential toxicity [16]. In particular, these first studies, focused mainly on inhalation and dermal exposure, revealed a pulmonary [17–19] and dermal [20–22] toxicity. The data currently available are insufficient for a conclusive risk assessment. Little is known about the features of CNT that determine their toxicity. Among the possible determinants there are the overall number of particles, the size, the surface area, the shape, the contaminants but also other physical and chemical properties. The literature lacks systematic production and elaboration of these data. For this reason, in this study we performed a comparative study of the bio-effects of three types of CNT with different properties.

We selected three different types of CNT, including: (a) CNT synthesized by an electric arc discharge in helium [23–26] composed of 50% multi-walled CNT (MWCNT) (10–40 nm large, 1–5 μm long) +30% single-walled CNT (SWCNT) (1–2 nm), the residual 20% containing fullerene and amorphous C as contaminants; (b) MWCNT produced by the CVD method, of larger size (110–170 nm × 5–9 μm), which contain 0.1% iron as a chemical contaminant; and (c) SWCNT produced by the CVD method, of smaller size (0.7–1.2 nm × 2–20 μm), which contain 1% Co and 1% Mo as chemical contaminants. Carbon black (CB) nanoparticles were used as reference particles with known biological properties.

We analyzed the effects of these different CNT on human tumor T lymphocytes (Jurkat cells), a well-known model of toxicological analysis. Nanoparticles can enter the blood stream upon inhalation, accidental bruises, and may possibly be purposely injected in the future for drug delivery. Thus, blood cells may be potential targets of CNT and the effects must be analyzed [16, 27–29].

The growing interest in the influence of CNT on human health has led to study their effect on cell death. Two different types of cell death exist: apoptosis, a cell-intrinsic mechanism that leads cells with mild damage to choose self-elimination [29, 30], or primary necrosis, a non-programmed and passive death caused by severe damage, characterized by dramatic and crucial changes in metabolism and structure [31–33]. Apoptotic cells, unlike necrotic ones, possess a still-functional energy metabolism and maintain plasma membrane integrity. As a last step, apoptotic cells lose energy and plasma membrane integrity by a process known as secondary necrosis, representing the necrotic stage of apoptosis. Secondary necrosis does not occur *in vivo* since apoptosizing cells are readily removed by phagocytes, thus disappearing without releasing their highly pro-inflammatory intracellular content. Apoptosis frees the organism from retention of potentially dangerous mutated or transformed cells. A deregulation of apoptosis leads to numerous pathologies: an increase of apoptosis leads to tissue degeneration (i.e. AIDS, Alzheimer's, Parkinson's disease), whereas a decrease leads to a hyper-proliferative disorder (i.e. autoimmune pathologies, viral infection, tumors) [34]. The goal of anti-cancer therapy is to induce apoptosis on tumor cells. In many pathological conditions, such as phagocytic deficit or massive production of apoptotic cells (i.e. due to cytocidal therapies), apoptosizing cells may accumulate and reach the secondary necrosis phase, thus leading to inflammation [35]. Alterations in apoptosis, secondary necrosis or primary necrosis have several implications, thus recommending that potential effects of CNT on cell death be investigated. As far as the proposed applications of CNT in drug delivery there is no information in the literature on the potential CNT effect on chemotherapic-induced apoptosis.

Numerous studies revealed that a direct physical interaction between CNT and cells exists. This physical interaction may produce an alteration on plasma membrane, and in particular changes in plasma membrane potential, a parameter controlled by specific ion pumps and responsible for cell homeostasis. In some cell types, changes in membrane potential may alter cell behavior or survival mediating receptor-induced release of intracellular proteins [36], influencing the kinetics of different active transport processes [37, 38] or interfering with ion transport by affecting the transport affinity [39, 40]. A literature search did not identify any studies that focused on the relationship between plasma membrane potential and CNT exposure.

In the present study we provide evidence that the three different types of CNT examined are directly cytotoxic on Jurkat cells. They alter the rate of cell transition from apoptosis to secondary necrosis and induce a plasma membrane hyperpolarization in a time-dependent way. CNT also increase damaging/chemotherapic-induced apoptosis. The comparative analysis of physical and chemical properties of the different CNT studied revealed that the toxic effect is determined by the shape, the size, the chemical contaminants and the concentration, which we thus propose as the parameters that need to be explored in order to identify the potential toxic effect of CNT.

2. Materials and methods

2.1. Nanomaterials

Four different types of carbon nanomaterial were examined in this study.

Two are different types of commercially available CNT. These nanotubes were produced using chemical vapor deposition and still contain some metal catalyst impurities. The first were MWCNT. Their diameter is in the range 110–170 nm while their length is between 5 and 9 μm. 0.1% of Fe is present in this sample (figure 1). The second were SWCNT. Their diameter is in the range 0.7–1.2 nm while their length is between 2 and 20 μm. 1% of Co and 1% di Mo are present in this sample (figure 2). Both were purchased from Sigma-Aldrich.

In order to analyze the influence of metal catalyst impurities, CNT with no metal contaminants were also examined. This third type of CNT used was synthesized by an arc discharge between two pure graphite electrodes at 24 V and 110 A, under a pressure of 600 Torr of helium (ADP-CNT arc

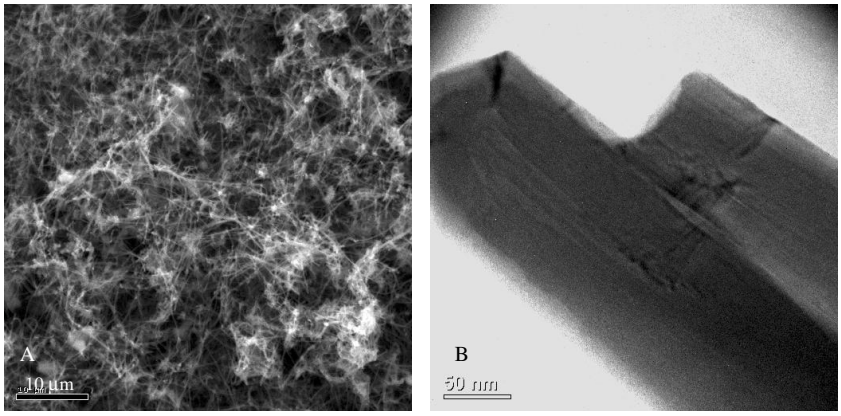

Figure 1. Electron microscopy images of the MWCNT produced by CVD. (A) SEM image. (B) TEM image.

Table 1. Main features of CNT preparations.

Type	Dimensions (diameter × length)	Density (g cm^{-3})	Surface area (m^2 g^{-1})	Synthesis	Contaminants
MWCNT	110–170 nm × 5–9 μm	1.35	1.3×10^2	CVD	Fe $< 0.1\%$
SWCNT	0.7–1.2 nm × 2–20 μm	2.25	1.7×103	CVD	Co $\sim 1\%$ Mo $\sim 1\%$
ADP-CNT[a]	10–40 nm × 1–5 μm	ND	ND	Electrical arc discharge	None

[a] ADP-CNT are a mixture of approximately 30% SWCNT, 50% MWCNT, 20% amorphous C and fullerene. The dimensions refer to the MWCNT component. ND: not determined.

discharge produced). Typical duration times were 3 min. This sample of ADP-CNT is composed of 50% of MWCNT, 30% of SWCNT (with a diameter of 1–2 nm) and 20% of amorphous C and fullerene. These ADP-CNT form bundles with a diameter in the range 10–40 nm, and their lengths are in the range 1–5 μm [23–26] (figure 3). Table 1 shows the main features of CNT examined.

Carbon black (CB) nanoparticles (Printex 90) donated by Degussa were used to compare the results obtained with CNT.

All nanomaterials were dispersed in tissue culture complete medium, sonicated (3–4 min), then vortexed (4–5 min) to get homogeneous suspensions and used immediately.

25 and 100 μg ml^{-1} of each of the four nanomaterial types were added to the cell culture.

2.2. Cell culture

Jurkat (human tumor T lymphocytes) cells were cultured in RPMI 1640 medium supplemented with 10% fetal calf serum (FCS), 2 mM L-glutamine, 100 IU ml^{-1} penicillin and streptomycin, kept in a controlled atmosphere (5% CO_2) and incubated at 37 °C. The experiments were performed on cells in the logarithmic phase of growth, in conditions of excellent viability, as assessed by trypan blue exclusion, $\geqslant$98%.

2.3. Analysis of cell proliferation

The number of viable cells was estimated in a hemocytometer at the times indicated.

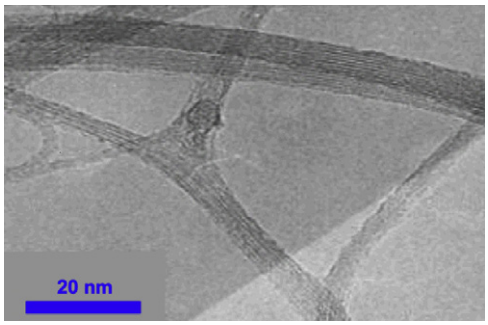

Figure 2. TEM image of the SWCNT produced by CVD.

2.4. Analysis of apoptosis

For the detection of apoptosis, cells were stained with the DNA-specific, cell-permeable dye Hoechst 33342 (Calbiochem), at a concentration of 10 μg ml^{-1}. Apoptotic cells were recognized according to their nuclear morphology (different stages of nuclear fragmentation) [41, 42].

Apoptosis was quantified as previously described [42]. Briefly, the fraction of Jurkat cells with fragmented nuclei among the total cell population was calculated in the Hoechst 33342 stained cells, counting at least 300 cells in at least ten randomly selected fields.

2.5. Analysis of primary/secondary necrosis

For the detection of necrosis, cells were stained with the cell-impermeable dye propidium iodide (PI) at a concentration of

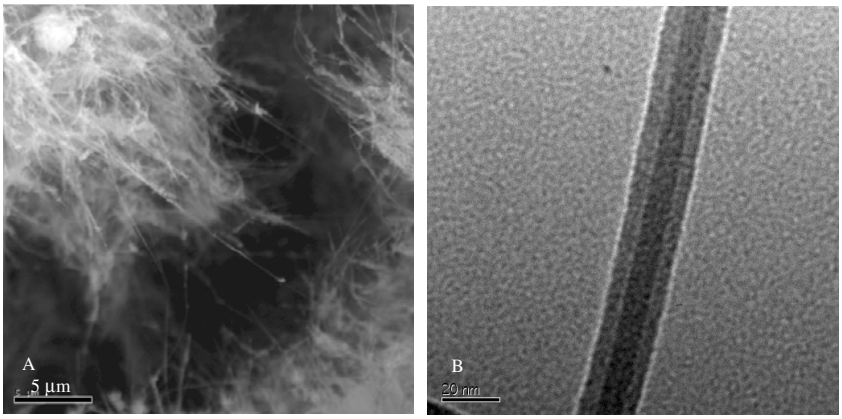

Figure 3. High-resolution electron microscopy images of the ADP-CNT samples. (A) SEM image. (B) TEM image.

5 μg ml^{-1} (Sigma-Aldrich). Necrotic cells were recognized according to their inability to exclude PI [43].

Necrosis was quantified as the fraction of Jurkat cells that uptake propidium iodide (PI) among the total cell population, counting at least 300 cells in at least ten randomly selected fields.

Primary versus secondary necrosis was discriminated by staining cells simultaneously with Hoechst 33342 and PI. Cells unable to exclude PI with fragmented or in shrinkage nuclei were recognized as cells in secondary necrosis, whereas cells unable to exclude PI with swollen nuclei were recognized as cells in primary necrosis.

2.6. Analysis of plasma membrane potential

For the detection of plasma membrane potential, cells were stained with the 5 μM anionic oxonol dye bis-(1,3-dibutylbarbituric acid) trimethine oxonol DiBAC (Molecular Probes, Eugene, OR, USA) at 37 °C for 15 min in the dark. Cells were stored at room temperature for 20 min before the measurements. Hyperpolarization causes extrusion of the dye so decreased fluorescence, whereas depolarization causes an increase in fluorescence [44].

2.7. Induction of apoptosis

Apoptosis was induced with the protein synthesis inhibitor puromycin (SIGMA, PMC, 10 μg ml^{-1}) or with the topoisomerase II inhibitor etoposide (SIGMA, VP16, 100 μg ml^{-1}). All compounds were kept throughout the experiments.

2.8. Flow cytometric measurements

Measurements of plasma membrane potential were performed with a FACScalibur (Becton Dickinson, San Jose, CA, USA) flow cytometer, equipped with a 488 nm laser. DiBAC emission was detected at 535 nm. Data were recorded for further analysis with Cell Quest software (Becton Dickinson, Franklin Lakes, NJ, USA). The mean fluorescence value was determined by counting 10 000 cells.

For comparison between different experiments, the value of each treated cell sample was compared with the value of the control cell sample, which was considered equal to 100. The values were then given as a fold increase with respect to the control.

2.9. Fluorescence microscopy and digital photomicrography

For fluorescence microscopy analysis stained cells were observed in fluorescence microscopy using a Nikon Eclipse TE200 microscope equipped with a 100 W mercury lamp. Images were recorded with a Cool SNAP digital camera.

2.10. Statistical analysis

Statistical analyses were performed using Student's t-test for unpaired data and p values <0.05 were considered significant. Data are presented as mean $\pm$ SD (standard deviation).

3. Results

3.1. Cytotoxic effects of carbon nanotubes

First of all, we explored whether incubation with carbon nanoparticles might reduce the cell viability. Thus, we analyzed the extent and type of cell death. In figure 4 we report the extent of total cell death (apoptosis or necrosis) found in the cultures exposed to 25 or 100 μg ml^{-1} of ADP-CNT, MWCNT, SWCNT and CB for 1–3 days.

The incubation with carbon nanoparticles induced a direct cytocidal effect on Jurkat cells, since a significant increase in cell death was detectable with all of the carbon nanoparticles examined. The extent of the cytotoxic effect was concentration- and time-dependent for each type of carbon nanoparticles. The most pronounced effect was associated with SWCNT, the smallest nanomaterial tested, and it was closely followed by MWCNT. These are the nanomaterials that contain metal contaminants. The minor cytotoxic effect was associated with CB.

Then, we analyzed the type of cell death induced by carbon nanoparticles. Independently of the type, these carbon nanoparticles, with their different properties, did not induce primary necrosis over the basal level (around 1%, always found in Jurkat cultures) up to 24 h of exposure. They induced

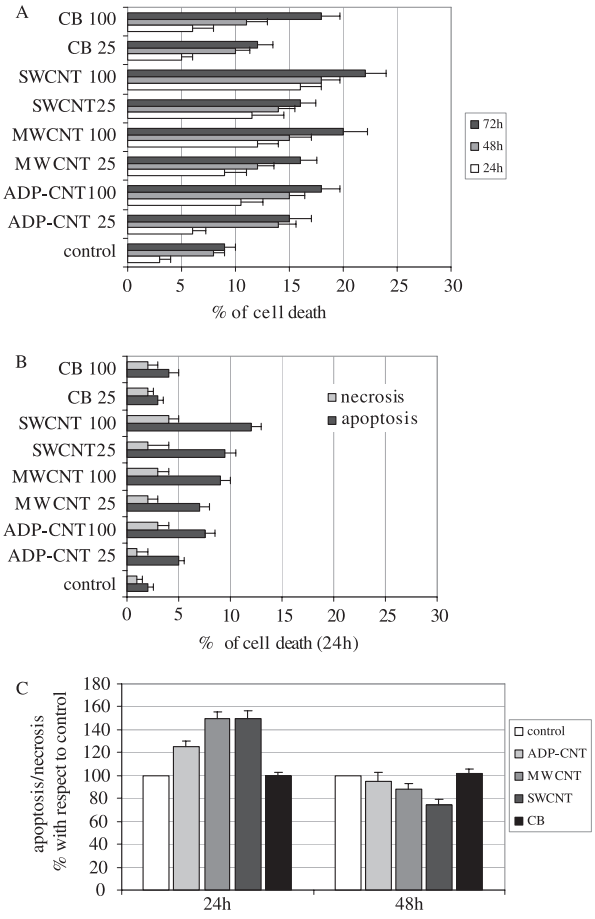

Figure 4. CNT on cell death of Jurkat cells. (A) The extent of cell death (apoptosis plus necrosis) measured in the cultures exposed to 25 or 100 μg ml^{-1} ADP-CNT, MWCNT, SWCNT and CB, at 24, 48 and 72 h. (B) The extent of apoptosis and secondary necrosis found in the cultures exposed to the different types and concentrations of carbon nanoparticles for 24 h. (C) The ratio between the extent of apoptosis versus the extent of secondary necrosis found in the cultures exposed to 100 μg ml^{-1} of the different carbon nanoparticles for 24 and 48 h. The values are in percent with respect to control. The values are the average of three measurements for each CNT concentration $\pm$ SD.

apoptosis, which *in vitro* evolves into secondary necrosis. In figure 4(B) we reported the extent of apoptosis and secondary necrosis found in the cultures exposed to the different types and concentrations of carbon nanoparticles for 24 h. The extent of apoptosis and of secondary necrosis increased in parallel, in a concentration- and time-dependent fashion for each type of carbon nanoparticle. The extent of apoptosis was always major with respect to the extent of secondary necrosis for all types of carbon nanoparticles examined at 24 h.

In figure 4(C) we reported the ratio between apoptosis versus secondary necrosis found in the cultures exposed to 100 μg ml^{-1} of the different carbon nanoparticles for 24 and 48 h. At 24 h the sample exposed to carbon nanotubes (ADP-CNT, MWCNT and SWCNT) showed a ratio apoptosis/necrosis higher with respect to control cells. Thus, at 24 h carbon nanotubes slowed down the rate of cell transition from apoptosis to secondary necrosis. This effect is time-dependent because at 48 h we observed an opposite behavior. At 48 h the ratio apoptosis/necrosis lowers in cultures exposed to carbon nanotubes (ADP-CNT, MWCNT and SWCNT) with respect to the control cells. Thus, at 48 h carbon nanotubes accelerated the rate of cell transition from apoptosis to secondary necrosis. The carbon black did not alter the apoptosis/necrosis ratio.

3.2. Carbon nanotubes do not affect Jurkat proliferation

Next, we analyzed the effect of CNT exposure on the proliferation of Jurkat cells.

Cells were incubated with 25 or 100 μg ml^{-1} of each carbon nanoparticle, and cell numbers were evaluated by means of hemocytometric analysis for 3 d, and compared with control cells. Exposure to CNT does reduce the number of cells exposed to carbon nanomaterial with respect to untreated cells (not shown), but the decrease is due to cell loss (see cell death in figure 4) rather than a direct effect on the proliferation rate, since the profile of the growth curves complements the profile of the cell death curves ADP-CNT (not shown). Thus, these types of carbon nanoparticles did not affect Jurkat proliferation.

3.3. Carbon nanotubes do not induce gross morphological alterations in Jurkat cells

Jurkat cells untreated or exposed for 4 h to 100 μg ml^{-1} of the four different types of carbon nanomaterials were analyzed by phase contrast optical microscopy. The microscopic analysis of the cells exposed to the different carbon nanomaterials revealed the existence of a direct physical interaction between cells and aggregates of carbon nanomaterials (figure 5), evident as black spots on some of the cells. For figure 5 we selected cells that display a peculiar arrangement around agglomerates of carbon nanomaterials. We want to stress that such aggregates are quite rare, and most cells are devoid of microscopically detectable CNT aggregates, even though we cannot exclude that free CNT, undetectable by optical microscopy, are indeed close to the cells. The observation of the cells revealed that no morphological alterations are detectable by phase contrast microscopic analysis in cells exposed to the different carbon nanomaterials (figure 5, left column). The analysis of cells stained with Hoechst 33342 (figure 5, central column) revealed that the cells that interact with CNT have a normally shaped nucleus, with regularly relaxed chromatin, very much like the control cells. At 4 h we did not observe apoptosis.

3.4. Carbon nanotubes induce plasma membrane hyperpolarization in Jurkat cells

We next analyzed the effect of CNT exposure on plasma membrane of Jurkat cells. Cells were stained with the fluorescent probe DiBAC, which specifically measures plasma membrane potential. Increased DiBAC fluorescence intensity indicates plasma membrane depolarization, whereas decreased fluorescence indicates plasma membrane hyperpolarization. We found that, in Jurkat cells, 3 h of exposure to CNT did not induce plasma membrane potential alteration (figure 5,

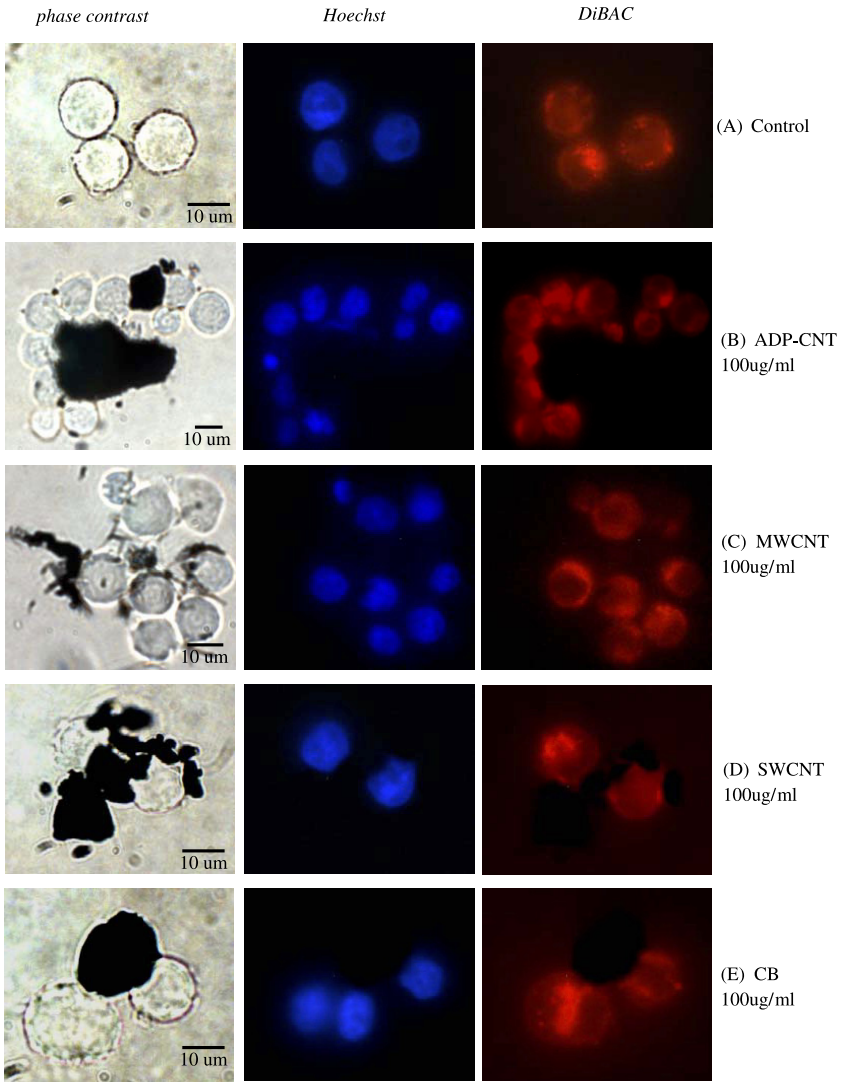

Figure 5. Morphology of Jurkat cells incubated with carbon nanotubes. Jurkat cells were incubated for 3 h with 100 μg ml^{-1} of CNT and cell. Nuclear morphology and plasma membrane potential were analyzed. No morphological alterations due to CNT were observed in the phase contrast analysis (left column). (A) Control cells; (B) cells exposed to ADP-CNT; (C) cells exposed to MWCNT; (D) cells exposed to SWCNT; (E) cells exposed to CB. The peculiar arrangement of cells around large aggregates of CNT were selected; though rare (see text), they show the direct physical interaction between cells and CNT. Nuclear morphology is unambiguously revealed by Hoechst 33342 staining (central column). Cells that interact with carbon nanoparticles (B)–(E) show normal nuclear morphology, with no condensed chromatin, as in control cells (A). The Hoechst panels show that all cells are viable (i.e. apoptosis not detectable). Plasma membrane potential was revealed by DiBAC staining (right column). Cells that interact with carbon nanoparticles (B), (D) and (E) show plasma membrane potential the same as control cells (A). The DiBAC panels show lack of plasma membrane potential alteration at 3 h of CNT exposure.

right column). Interestingly, a kinetics analysis shows that at 24 h CNT induce a strong plasma membrane hyperpolarization (figure 6(A)), which increases in a concentration-dependent way. The most pronounced effect was associated with SWCNT, and it was closely followed by MWCNT; the weakest effect was associated with CB.

This alteration is not an immediate consequence of the physical interaction between CNT and cells, since it was not found at early time points, thus suggesting that it is the result of an intracellular signaling process. We can also exclude that it is the result of a gross interaction with the aggregates, since the flow cytometric analysis indicates that it occurs in all cells, as shown by the unique peak (figure 6(B)), though we cannot exclude a general interaction with free, sub-microscopic CNT.

3.5. CNT increase stress-induced apoptosis

The incubation with nanotubes induces a significant effect in the modulation of apoptosis induced by damaging agents such as PMC or VP16. In figure 7 we report the extent of apoptosis induced by PMC upon 24 h of exposure with the different types and concentrations of carbon nanomaterial. The value reported indicate the extent of apoptosis due to PMC, for which we subtracted the extent of apoptosis directly induced by each type of CNT.

Interestingly, all the nanotubes tested (ADP-CNT, MWCNT and SWCNT) increase the extent of PMC-induced apoptosis. CB did not affect stress-induced apoptosis. Similar results were observed with VP16 (not shown).

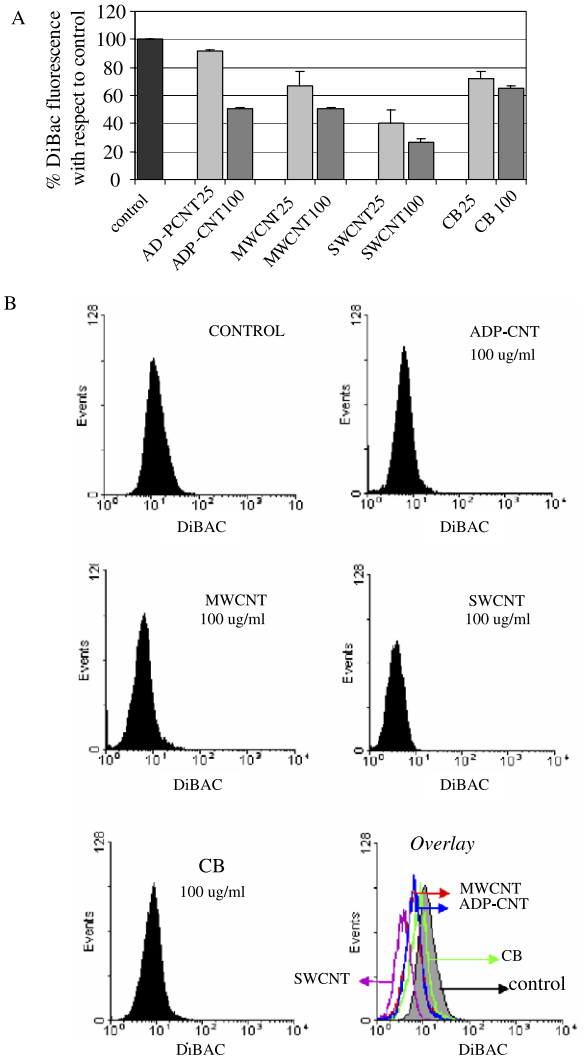

Figure 6. CNT alter plasma membrane potential. Flow cytometric analysis of plasma membrane potential of Jurkat cells after 24 h of incubation with 25 or 100 μg ml^{-1} of ADP-CNT, MWCNT, SWCNT and CB. Plasma membrane potential was revealed by DiBAC staining. (A) The values were given as percent with respect to control. The values are the average of four experiments $\pm$ SD. (B) The analysis of flow cytometric histograms reveals that carbon nanoparticle-treated cells distribute as a unique peak: the decrease of DIBAC fluorescence affects all cells. One of four different experiments with similar results is shown. The last histogram shows the overlay of the histograms of control cells (in gray), cells exposed to ADP-CNT (in blue), cells exposed to MWCNT (in red), cells exposed to SWCNT (in violet) and cells exposed to CB (in green) (or see arrows in place of colors).

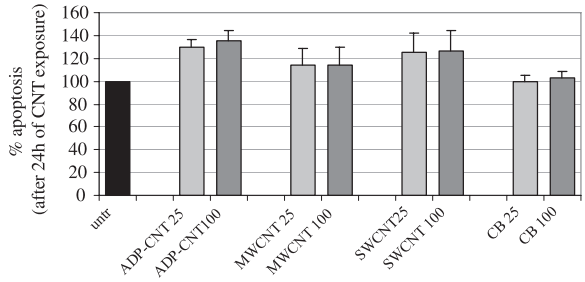

Figure 7. CNT increase apoptosis induced by stress agent on Jurkat. Jurkat cells after 24 h of incubation with 25 or 100 μg ml^{-1} of the different carbon nanomaterials were induced to apoptosis with PMC. Apoptosis was measured at 4 h of PMC. The values reported indicate the extent of apoptosis; the extent of apoptosis directly induced by each different CNT was subtracted. Values are the average of at least five experiments for each treatment $\pm$ SD.

4. Discussion

We show here that exposure to CNT increases the incidence of apoptosis of Jurkat cells; this supports previous observations showing that CNT induce apoptosis on the T lymphocytic cells Jurkat [29]; we also report the novel finding that CNT did not increase the frequency of primary necrosis. However, after 48 h CNT accelerated the rate of cell transition from apoptosis to secondary necrosis. Potential pathological consequences may occur when the process of apoptosis is accelerated and the cells may prematurely enter the necrotic stage. The cells may not have adequate time to form apoptotic bodies to be phagocytozed and safely eliminated by phagocytes. In these cases, the probability of inflammatory and autoimmune reactions, due to secondary necrotic cell lysis and release of cell content into the intercellular space, increases. By modulating the incidence and the speed of apoptosis, CNT may exert an effect on inflammation, autoimmunity and pathologies characterized by loss of cell homeostasis.

The simultaneous exposure to CNT and to the chemotherapic- or stress-inducer apoptosis increases the extent of apoptosis. This is a result in favor of potential application of CNT in drug delivery, but at the same time suggests the possibility of a health risk of CNT in conditions in which damage is accidental (i.e. solar UV light) and not induced pharmacologically.

Our present finding showed, for the first time, that CNT induce a plasma membrane potential alteration. In Jurkat cells, after 24 h of exposure, CNT induce a plasma membrane hyperpolarization. Plasma membrane polarity is a function of the intracellular energy asset, controlling the extracellular/intracellular exchanges of information; thus, a change in PMP is suggestive of a change in cell behavior but has nothing to do with toxicity, since PMP alterations do not lead to loss of PM integrity. Indeed, at 24 h the cell incubated with CNT show a hyperpolarized but functional plasma membrane, since they are able to exclude the PI.

The mechanism by which plasma membrane potential is affected by CNT is still to be explored. Previously, we reported that the same types of CNT did not significantly affect cell viability on tumor human monocytes cells, U937 [45]. Thus, if Jurkat cells may be defined as 'sensitive' to the modulation of apoptosis by CNT, U937 are instead 'insensitive'. This indicates that the toxicological effect of CNT depends on cell type. It is known that alterations of membrane potential can modulate activity of Ca^{2+} channels, inducing Ca^{2+} fluxes through voltage-dependent membrane channels [46]. Interestingly, Ca^{2+} influx has opposite effects on the viability of Jurkat versus U937 cells. In Jurkat cells Ca^{2+} influx is a trigger for apoptosis [47]. Instead, in U937 cells Ca^{2+} influx has an opposite, anti-apoptotic effect [48]. Our results show

that in Jurkat cells CNT exposure induces plasma membrane hyperpolarization and apoptosis, thus suggesting that CNT bio-effects may be mediated by a mechanism involving Ca^{2+} entry into cells, and we are presently investigating the effects of CNT on intracellular Ca^{2+} parameters.

Interestingly, our results show that plasma membrane hyperpolarization is not an immediate consequence of the physical interaction between CNT and cells, since at early time points (3 h) it is not detectable. Instead, it becomes apparent at later times (24 h), suggesting that it is an indirect consequence of the exposure to CNT. Many logical explanations to such a finding may be hypothesized. Among these, we want to mention the recently discovery of spontaneous functionalization of CNT in biological fluids [49]. In culture media, especially in the presence of fetal calf serum, electrophilic biomolecules (amino acids, vitamins, etc) bind to CNT, sheltering them from the environment. This may alter the culture media by depauperation of necessary nutrients. It will be interesting to test whether the hyperpolarization found in our experiments might be due to CNT-induced medium depauperation.

We found that the most pronounced effects on apoptosis and plasma membrane potential were associated with SWCNT, and it was closely followed by MWCNT. SWCNT, the most effective, were the smallest nanomaterials tested. This result supports the finding that SWCNT are more toxic than MWCNT [50]; moreover, it points out the importance of surface area and small dimensions in cellular toxicity. As expected, CB was the least effective. Thus, it was the material structure in CNT that strongly induced alteration in cell behavior. However, we have to keep in mind that SWCNT and MWCNT contain metal contaminants. Catalytic metals like iron, molybdenum and cobalt may be toxic at high concentration [51, 52], and may increase the real toxic effect of CNT. The comparison of the effects of the sample of CNT with (MWCNT and SWCNT) or without (ADP-CNT and CB) catalytic metals helped us to evaluate the toxic effects of these new materials versus the contaminants.

In conclusion, the results of our comparative study of toxicological effects and physico-chemical properties of CNT reveal that shape, size, chemical contaminants and concentration are all parameters that influence CNT biological effects. Thus, the main message from this study is that CNT, independently of the type of preparation and presence of contaminants, deeply affect cell behavior.

With this study we mean to contribute to the important toxicological screening strategy necessary to identify the potential toxic effect of CNT, and thus to prevent expose risk and develop safe biomedical applications.

Acknowledgments

The work was partially supported by grants from the Italian Ministry of University and Scientific Research (PRIN grant no. 2006069554). Ultrafine Carbon Black (CB) nanoparticles (Printex 90™, 14 nm diameter) were a generous gift of Degussa Italia SpA, Advanced Fillers and Pigments, Ravenna, Italy. We gratefully acknowledge Professors A Bergamaschi and A Magrini for their interest in this work.

References

[1] Niu C, Sichel K, Hoch R, Moy D and Tennent H 1997 *Appl. Phys. Lett.* **70** 1480–2
[2] Bower C, Rosen R, Lin J, Han J and Zhou O 1999 *Appl. Phys. Lett.* **74** 3317–9
[3] Cheng Y and Zhou O 2003 *C. R. Physique* **4** 1021–33
[4] Lam C W, James J T, McCluskey R, Arepalli S and Hunter R L 2006 *Crit. Rev. Toxicol.* **36** 189–217
[5] Martin C R and Kohli P 2003 *Nat. Rev. Drug Discov.* **2** 29–37
[6] Lacerda L, Bianco A, Prato M and Kostarelos K 2006 *Adv. Drug. Deliv. Rev.* **58** 1460–70
[7] Banerjee S, Kahn M G and Wong S S 2003 *Chemistry* **9** 1898–908
[8] Bottini M, Tautz L, Huynh H, Monosov E, Bottini N, Dawson M I, Bellucci S and Mustelin T 2005 *Chem. Commun.* 758–60
[9] Bianco A, Kostarelos K and Prato M 2005 *Curr. Opin. Chem. Biol.* **9** 674–9
[10] Bottini M, Balasubramanian C, Dawson M I, Bergamaschi A, Bellucci S and Mustelin T 2006 *J. Phys. Chem.* B **110** 831–6
[11] Donaldson K, Aitken R, Tran L, Stone V, Duffin R, Forrest G and Alexander A 2006 *Toxicol. Sci.* **92** 5–22
[12] Bottini M, Magrini A, Di Venere A, Bellucci S, Dawson M I, Rosato N, Bergamaschi A and Mustelin T 2006 *J. Nanosci. Nanotechnol.* **6** 1381–6
[13] Klumpp C, Kostarelos K, Prato M and Bianco A 2006 *Biochim. Biophys. Acta.* **1758** 404–12
[14] Meng J, Song L, Meng J, Kong H, Zhu G, Wang C, Xu L, Xie S and Xu H 2006 *J. Biomed. Mater. Res.* A **79** 298–306
[15] Zanello L P, Zhao B, Hu H and Haddon R C 2006 *Nano Lett.* **6** 562–7
[16] Borm P J A *et al* 2006 *Part. Fibre Toxicol.* **3** 11
[17] Lam C W, James J T, McCluskey R and Hunter R L 2004 *Toxicol. Sci.* **77** 126–34
[18] Warheit D B, Laurence B, Reed K L, Roach D H, Reynolds G A and Webb T R 2004 *Toxicol. Sci.* **77** 117–25
[19] Jia G, Wang H, Yan L, Wang X, Pei R, Yan T, Zhao Y and Guo X 2005 *Environ. Sci. Technol.* **39** 1378–83
[20] Shvedova A A, Castranova V, Kisin E R, Schwegler-Berry D, Murray A R, Gandelsman V Z, Maynard A and Baron P 2003 *J. Toxicol. Environ. Health* **66** 1909–26
[21] Ding L, Stilwell J, Zhang T, Elboudwarej O, Jiang H, Selegue J P, Cooke P A, Gray J W and Chen F F 2005 *Nano Lett.* **5** 2448–64
[22] Monteiro-Riviere N A, Nemanich R J, Inman A O, Wang Y Y and Riviere J E 2005 *Toxicol. Lett.* **155** 377–84
[23] Bellucci S 2005 *Phys. Status Solidi* c **2** 34–47
[24] Bellucci S 2005 *Nucl. Instrum. Methods* B **234** 57–77
[25] Bellucci S, Balasubramanian C, Micciulla F and Rinaldi G 2007 *J. Exp. Nanosci.* **2** 193–206
[26] Bellucci S, Balasubramanian C, Micciulla F and Tiberia A 2007 *J. Phys.: Condens. Matter* **19** 395014
[27] Dumortier H, Lacotte S, Pastorin G, Marega R, Wu W, Bonifazi D, Briand J P, Prato M, Muller S and Bianco A 2006 *Nano Lett.* **6** 1522–8
[28] Radomski A, Jurasz P, Alonso-escolano D, Drews M, Morandi M, Malinski T and Radomski M W 2005 *Br. J. Pharmacol.* **146** 882–93
[29] Bottini M, Bruckner S, Nika K, Bottini N, Bellucci S, Magrini A, Bergamaschi A and Mustelin T 2006 *Toxicol. Lett.* **160** 121–6
[30] Bohm I and Schild H 2003 *Mol. Imaging Biol.* **5** 2–14
[31] Coppola S and Ghibelli L 2000 *Biochem. Soc. Trans.* **28** 56–61
[32] Fiers W, Beyaert R, Declercq W and Vandenabeele P 1999 *Oncogene* **18** 7719–30
[33] Edinger A L and Thompson C B 2004 *Curr. Opin. Cell Biol.* **16** 663–9
[34] Fadeel B and Orrenius S 2005 *J. Intern. Med.* **258** 479–517

[35] Fadeel B 2003 *Cell Mol. Life Sci.* **60** 2575–85
[36] Frey J *et al* 1986 *Eur. J. Biochem.* **158** 85–9
[37] Eleno N, Deves R and Boyd C A 1994 *J. Physiol. Lond.* **479** 291–300
[38] Haslberger A, Romanin C and Koerber R 1992 *Mol. Biol. Cell* **3** 451–60
[39] Blatt M R, Rodriguez-Navarro A and Slayman C L 1987 *J. Membr. Biol.* **98** 169–89
[40] Oettgen H C *et al* 1985 *Cell* **40** 583–90
[41] Dini L, Coppola S, Ruzittu M T and Ghibelli L 1996 *Exp. Cell Res.* **223** 340–7
[42] De Nicola M, Gualandi G, Alfonsi A, Cerella C, D'Alessio M, Bergamaschi A, Magrini A and Ghibelli L 2006 *Biochem. Pharmacol.* **72** 1405–16
[43] Cerella C *et al* 2006 *Ann. New York Acad. Sci.* **1090** 50–8
[44] Nuccitelli S *et al* 2006 *Ann. New York Acad. Sci.* **1090** 217–25
[45] De Nicola M *et al* 2007 *J. Phys.: Condens. Matter* **19** 395013
[46] Lewis R S and Cahalan M D 1995 *Annu. Rev. Immunol.* **13** 623–53
[47] Tantral L, Malathi K and Kohyama S *et al* 2004 *Biochem. Pharmacol.* **22** 35–40
[48] Fanelli C, Coppola S, Barone R, Colussi C, Gualandi G, Volpe P and Ghibelli L 1999 *FASEB J.* **13** 2031–6
[49] Kam N W and Dai H 2005 *J. Am. Chem. Soc.* **127** 6021–6
[50] Tian F, Cui D, Schwartz H, Estrada G G and Kobayashi H 2006 *Toxicol. In Vitro* **20** 1202–12
[51] Anderson G J 2007 *Am. J. Hematol.* **82** 1128–31
[52] Evans E J and Thomas I T 1986 *Biomaterials* **7** 25–9